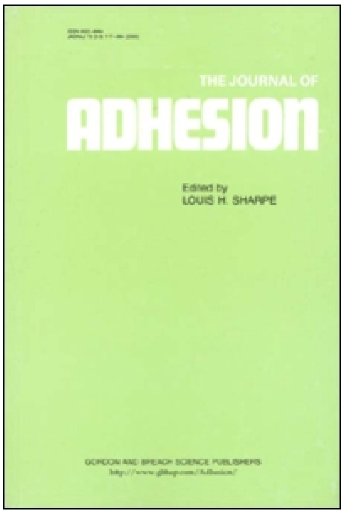

The Journal of Adhesion
Publication details, including instructions for authors and subscription information:
http://www.informaworld.com/smpp/title~content=t713453635

Photoelastic Determination of Flaw Size and Distribution Effects on Adhesively Bonded Lap Joints

C. L. Chow[a]; C. W. Woo[a]
[a] Department of Mechanical Engineering, University of Hong Kong, Hong Kong

To cite this Article Chow, C. L. and Woo, C. W.(1986) 'Photoelastic Determination of Flaw Size and Distribution Effects on Adhesively Bonded Lap Joints', The Journal of Adhesion, 19: 2, 89 — 111
To link to this Article: DOI: 10.1080/00218468608071216
URL: http://dx.doi.org/10.1080/00218468608071216

J. Adhesion, 1986, Vol. 19, pp. 89–111
0021–8464/86/1902–0089 $18.50/0

Photoelastic Determination of Flaw Size and Distribution Effects on Adhesively Bonded Lap Joints

C. L. CHOW and C. W. WOO

Department of Mechanical Engineering, University of Hong Kong, Pokfulam Road, Hong Kong

It is well known that the load carrying capacity of adhesively bonded lap joints can be influenced by the presence of flaw-like defects which are often created during its bonding process. To design an effective adhesive joint containing possible bonding defects, adequate knowledge and understanding of the shear stress distribution along the entire lap joint are necessary.

This paper describes an investigation into the effects of internal adhesive flaw size and distribution on the fracture behaviour of adhesively bonded lap joints. Photoelasticity is used to gain a quantitative understanding of the localized shear stress concentrations due to the presence of the internal flaws along the bonding layer. It is observed that a 20% increase in the maximum shear stress may be induced when an isolated central flaw of 5.0 mm was extended to 37.5 mm representing a flaw size of 75% of the lap length. For the presence of multiple flaws along the bonding line, there is no significant effect of the flaw separation distance on the maximum shear stresses. There is, however, a marked increase in the maximum shear stress up to about 45% when a flaw size is increased from 2.5 mm to 7.5 mm.

KEYWORDS: Adhesive bonding, flaw distribution, flaw size, fracture behavior, lap joints, photoelastic method.

1. INTRODUCTION

The mechanical properties of adherend and adhesive, joint geometry, surface preparation, bonding technique, testing method, etc. are known to have a definite influence on the load-bearing capability of adhesively bonded lap joints. To design an effective adhesive joint, the effects of the above mentioned parameters on the shear stress distribution along the adhesive bond-length need to be investigated and understood. It is therefore necessary to develop a simple yet effective method of determining the shear stress distribution along the lap joint.

Earlier investigators confined their stress analysis to the lap joint by assuming that the joint could be perfectly bonded free of any bonding defects.[1-10] In practice, adhesive joints do, however, contain flaw-like manufacturing defects introduced along the interface between the adhering surface and adhesive layer during the bonding process. These defects can induce stress concentrations and reduce the bonding strength. This observation has prompted recent investigators to take into account the significance of the bonding defects on the fracture strength of adhesive joints using the fracture mechanics approach.[11-19] All the fracture studies hitherto performed relating to the lap joints assumed that the defects, in the form of cracks, existed at the two lap ends where the highest stress concentrations are located. Bonding flaws observed in practice may not be confined at the lap ends but are randomly distributed along the bond line.

This paper is intended to study the effect of internal flaw size and its distribution along the adhesive layer on the fracture behaviour of adhesively bonded lap joints. This is achieved by examining the shear stress distribution developed along the lap joints with or without the presence of bonding flaws using the photoelasticity method.

2. EXPERIMENTAL ANALYSIS

2.1 Specimen Geometry and Material

The photoelastic models used for the investigation are depicted in Figure 1. The geometry of the specimens was specially designed so that the shear stress distribution along the adhesive joint can be measured.[8] The photoelastic material used was PSM-1 (Photolastic, Inc.) with a fringe value of 7.0 kN/fr/m (40 psi/fr/in), a Young's modulus of 2.35 GN/m^2 (340,000 psi) and a Poisson's ratio of 0.38. The adhesive employed was Rapid Araldite (CIBA) with hardner (H2951) to resin (AW4101) ratio of 10:8 by weight.

The bonding surfaces of the lap joint were carefully polished and cleaned before the adhesive was applied. An internal artificial flaw was 'implanted' in the bonding layer by placing a suitable thin layer of adhesive tape on the bonding surfaces (Figure 2c) before the adhesive was applied. The adhesively bonded photoelastic model was sub-

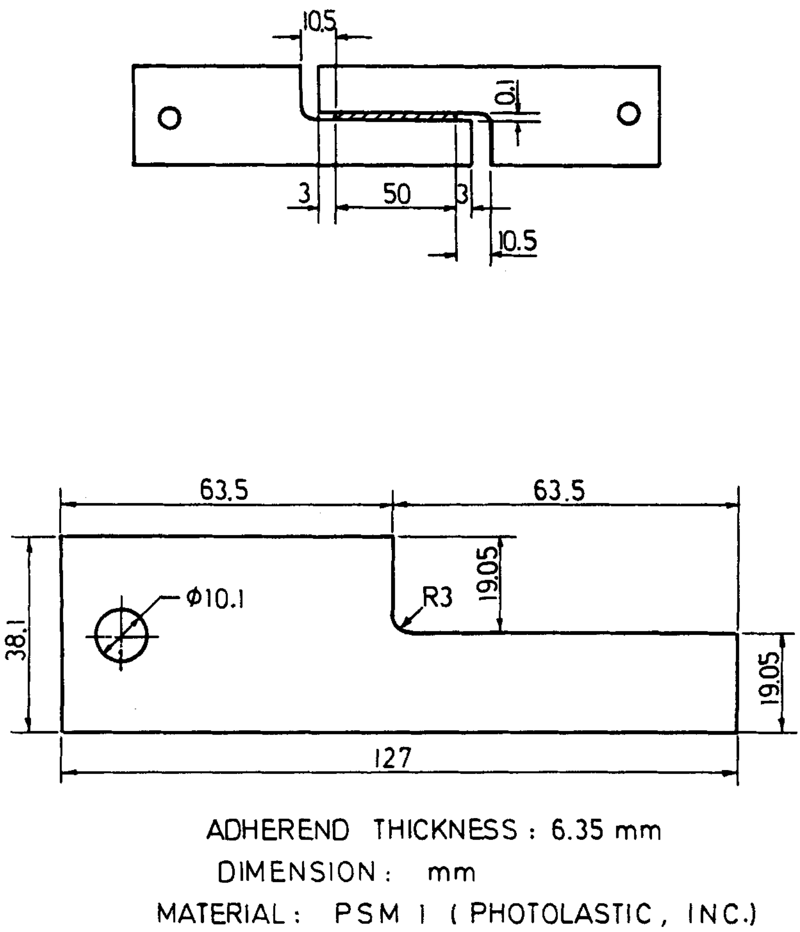

FIGURE 1

sequently heat-treated to remove any residual stresses that might have been produced during the bonding process.

In order to ascertain the bonding technique and the suitability of the adherend and adhesive materials used for this investigation, the shear stress distribution of an 'ideal' lap joint and of a 'perfect' adhesively

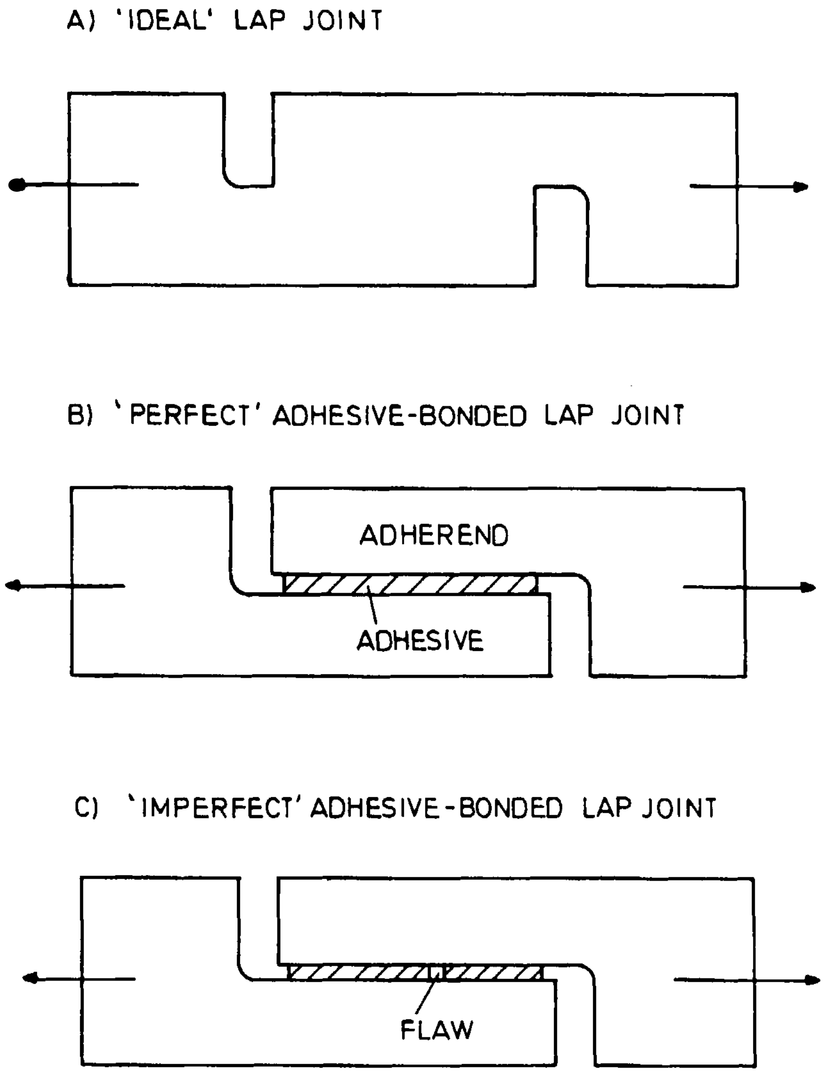
A) 'IDEAL' LAP JOINT
B) 'PERFECT' ADHESIVE-BONDED LAP JOINT
ADHEREND
ADHESIVE
C) 'IMPERFECT' ADHESIVE-BONDED LAP JOINT
FLAW

FIGURE 2

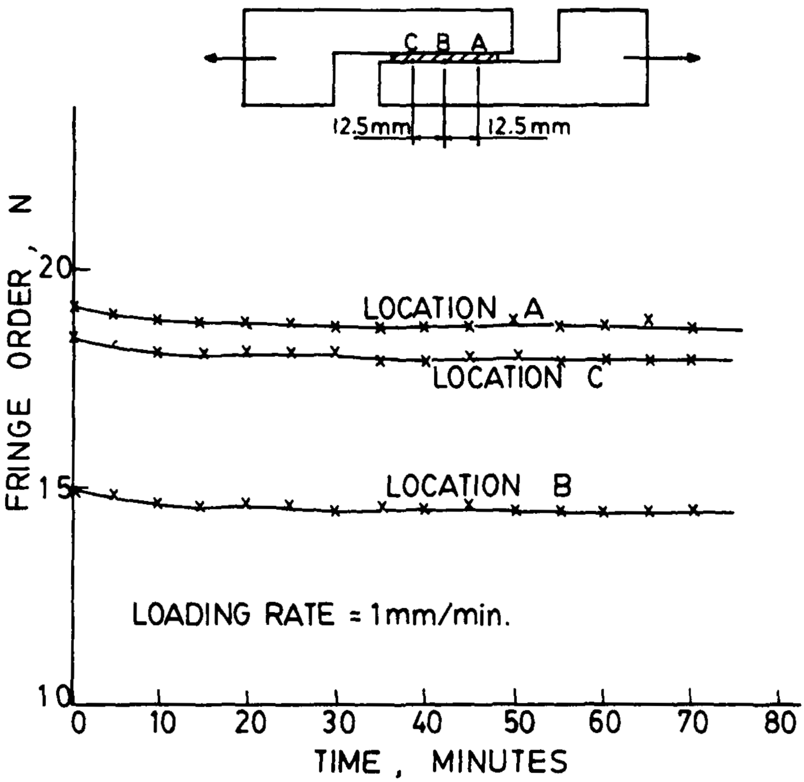

FIGURE 3

bonded lap joint were first analysed and compared. The 'ideal' lap joint has the same geometry of the bonded joint but is made of a single piece of photoelastic material as shown in Figure 2a. The 'perfect' adhesive joint as shown in Figure 2b is one which contains no implanted internal flaw-like defects or imperfections in the adhesive layer. All the test specimens were loaded within a loading frame placed between the bench-type transmission polariscope from which fringe developments were measured and recorded.

2.2 Creep and Relaxation

Creep and relaxation have been reported to have a definite effect on the fracture behaviour of adhesive joints.[20–23] A series of experiments was performed to examine the creep and relaxation characteristics of a 'perfect' lap joint (Figure 2b) in a room temperature of 15°C under an applied load of 178N (400 lb). For the lap joint length of 50 mm, maximum shear stress measurements (or fringe orders) were recorded at three

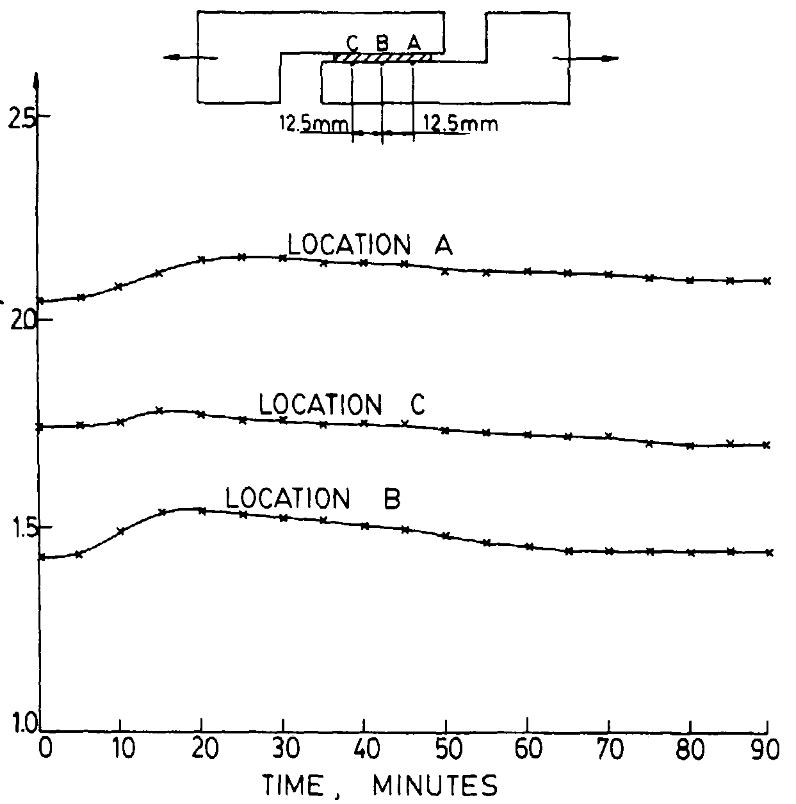

FIGURE 4

different locations, namely A, B, C, along the lap length as depicted in Figure 3. Location B refers to the mid-point of the bonded length whereas locations A and C refer to the points at 25% (or 12.5 mm) from the mid-point B.

It can be observed from Figure 3 depicting the measured creep characteristics along the interface of the lap joint that the creep effect is negligible up to the test period of about 80 minutes. A small decrease in the maximum shear stresses was observed up to about 10 minutes from the start of load application. The magnitude is, however, small and may fall well within the range of measurement uncertainties.

The relaxation characteristics of the lap joint were also measured and achieved by maintaining a constant displacement. The displacement was deduced by applying the same load of 178 N on the lap joint as the creep test. The maximum shear stress variation (or its equivalent fringe order) along the adherend and adhesive interface with time up to 90 minutes was recorded and shown in Figure 4. It can be observed from the figure that the measured fringe order increased initially due to the development of instantaneous elasticity and then decreased with time due to its

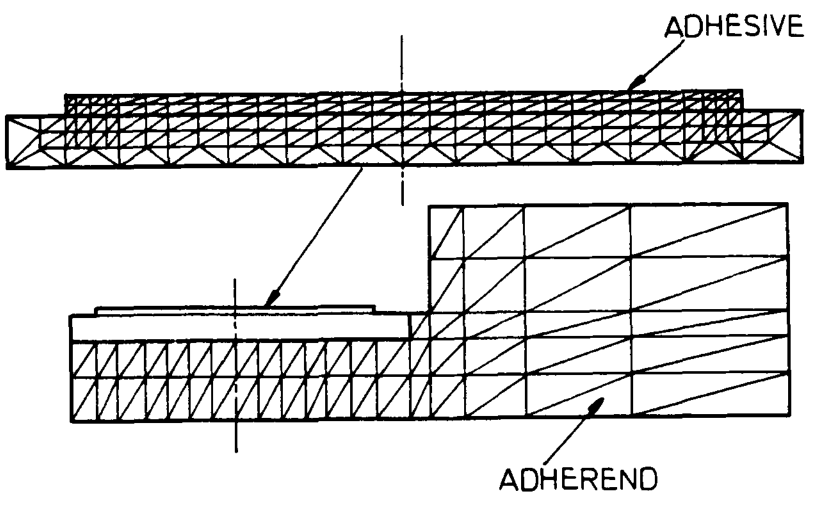

FIGURE 5

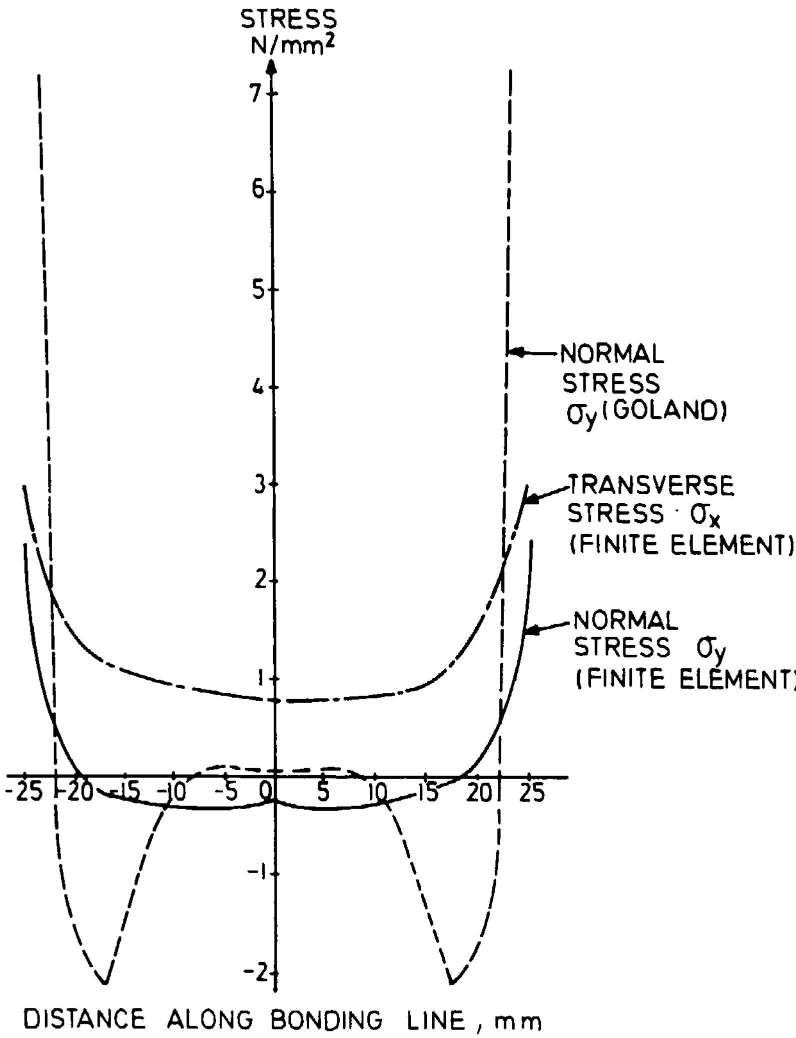
STRESS
N/mm²
7
6
5
4
3
2
1
-1
-2
-25 -20 -15 -10 -5 0 5 10 15 20 25
NORMAL
STRESS
σy (GOLAND)
TRANSVERSE
STRESS σx
(FINITE ELEMENT)
NORMAL
STRESS σy
(FINITE ELEMENT)
DISTANCE ALONG BONDING LINE, mm

FIGURE 6

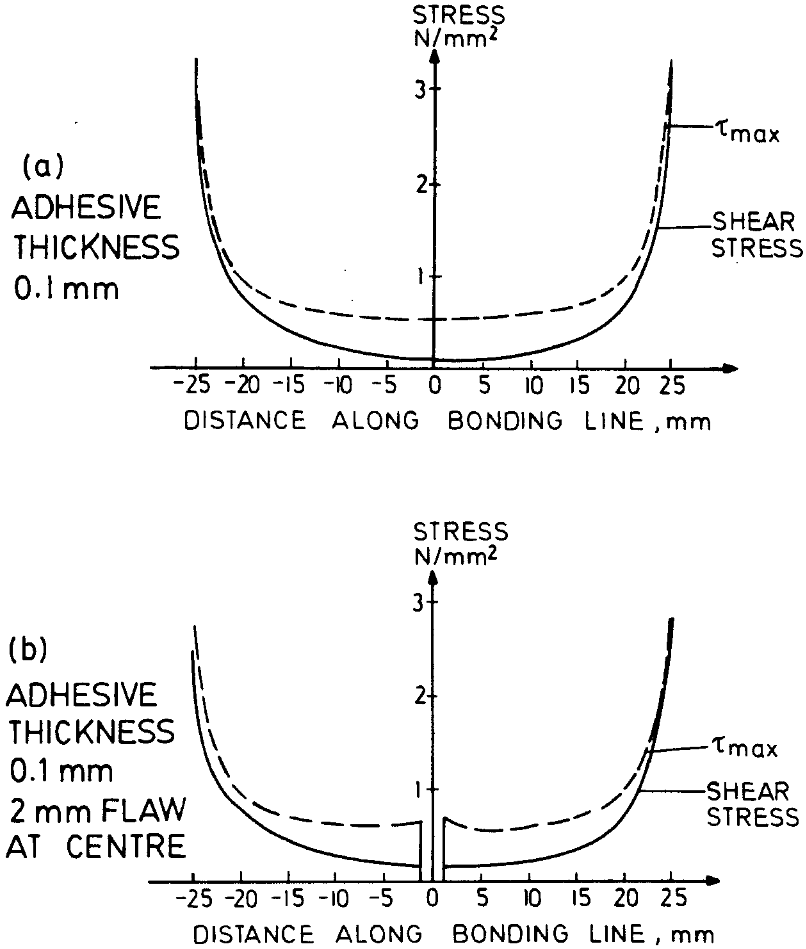

FIGURE 7

subsequent development of delayed elasticity. Similar phenomena in adhesive joints have been observed and reported elsewhere.[21–23]

In view of the observed creep and relaxation characteristics of the lap joint, all the measurements reported in the paper were taken about 15

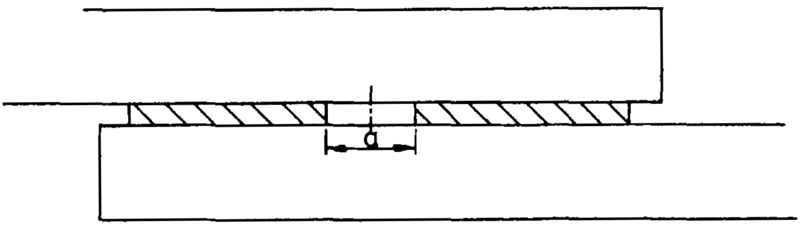

a = 5, 12.5, 25, 37.5 mm

(A) SINGLE CENTRAL ARTIFICAL FLAW

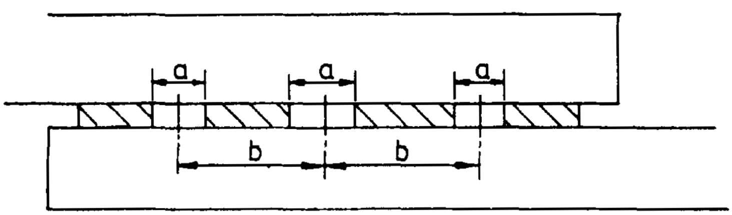

a = 2.5, 5, 7.5 mm

b = 12.5, 15, 17.5 mm

(B) THREE FLAWS SYMMETRICALLY SPACED

FIGURE 8

minutes after the load application of 178 N such that the creep and relaxation effects on the maximum shear stresses can be nullified.

2.3 Maximum versus True Shear Stress

One critical area in the lap joint fracture is the interfacial debonding between the adhering surface and adhesive layer. It is therefore important to distinguish between the 'true' shear stress and the maximum shear stress directly measurable from the photoelasticity along the joint interface. The specimen geometry depicted in Figure 1 was chosen by Renton[8] who concluded that the measured photoelastic maximum shear stresses from the specimen coincided with the true shear stresses along the bond line. This also implies that the lap joint geometry produces predominant transverse stress with negligible normal stress in the adhesive layer.

In an attempt to ascertain the extent to which the normal stresses induced by the lap geometry can be developed, a two dimensional finite element analysis was performed. Figure 5 depicts the lower half lap joint used for the computer model but the entire lap joint (including both upper and lower halves) was analysed. This was done to take into account any possible bending effects that may be induced due to the presence of the adhesive layer. For the finite element analysis, the constant strain triangular element was employed with a total of 295 nodal points and 534 elements. The Young's modulus and Poisson's ratio used are 2.35 GN/m^2 and 0.38 respectively for the adherend and the respective values for the adhesive are 1.91 GN/m^2 and 0.34.

Figure 6 shows the computed transverse stresses (σ_x) and normal stresses (σ_y) along the bonded length from the finite element analysis. It can be observed from the figure that although the normal stress may be considered insignificant for about 80% at the lap length, its magnitude is seen comparable to the transverse stress at two lap ends. Also shown in the figure is the separately computed normal stress based on Goland's formulation.[1] The Goland's results also confirm the presence of significant normal stresses for the lap joint geometry. The accuracy of the Goland's method is, however, far from satisfactory as compared with those by the finite element method because of simplifying assumptions made in the method for the sake of mathematical tractability.

The presence of normal stress is expected to produce significant difference in magnitude between the maximum shear stress and the true transverse shear stress (τ_{xy}) along the lap joint. This is confirmed in Figure

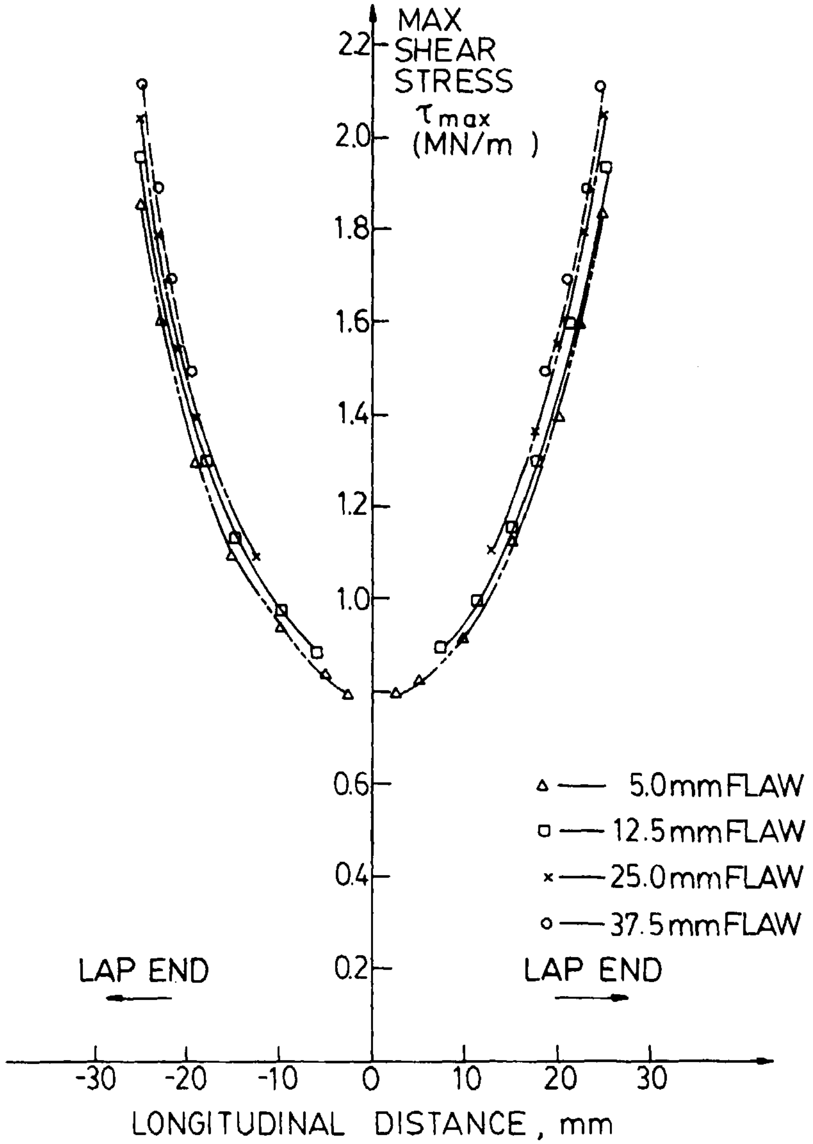
MAX
SHEAR
STRESS
τ_{max}
(MN/m)
2.2
2.0
1.8
1.6
1.4
1.2
1.0
0.6
0.4
0.2
5.0mmFLAW
12.5mmFLAW
25.0mmFLAW
37.5mmFLAW
LAP END
LAP END
-30
-20
-10
0
10
20
30
LONGITUDINAL DISTANCE, mm

FIGURE 9

7 for two types of lap joint. Figure 7a shows the computed maximum shear stress and the transverse shear stress (τ_{xy}) distributions for a 'perfect' lap joint and Figure 7b for an 'imperfect' lap joint embedded with a 2.0 mm central flaw. Both lap joints were bonded with 0.1 mm adhesive thickness and subjected to an applied load of 178 N.

It is of interest to note from Figure 7 that despite the observed difference in magnitude between the maximum and the transverse shear stresses, the profile or overall shape of the maximum shear stresses follows closely that of the transverse shear stresses along the entire lap joint. We may take advantage of this important observation to extend the applicability of the photoelasticity method for quantifying the governing parameters in the lap joint fracture studies.

The finite element analysis has been shown to produce satisfactory results in the study of adhesively bonded joints. The use of the method could, however, be proved to be time-consuming and expensive when the present investigation calls for the fracture characterization of lap joints embedded with randomly distributed flaws of varying sizes. To solve this class of problems, the photoelasticity method is considered to be comparatively more efficient and less time consuming.

3. RESULTS AND DISCUSSIONS

3.1 Photoelastic Analysis

As described in an earlier section, the bench type transmission polariscope was used to measure maximum shear stresses. The birefringent material of PSM-1 (Photolastic, Inc.) was chosen as adherend and bonded together with Rapid Araldite (CIBA) with an adhesive thickness maintained at 0.1 mm. Total lap length was 50 mm. Two types of artificial flaw were implanted along the adhesive layer. One is a single isolated central flaw of sizes 5 mm, 12.5 mm, 25 mm and 37.5 mm representing respectively 10%, 25%, 50% and 75% of the total lap length, Figure 8a. The second type is composed of three multiple flaws with varying combination of flaw size, a, and flaw separation distance, b, Figure 8b.

The shear stress distributions for the 'imperfect' bonded lap joint with various internal flaw sizes centrally located along the bonding length are shown in Figure 9. It can be observed from the figure that the shape of the maximum shear stress distribution is, as expected, similar for all the different flaw sizes. The larger the flaw size, the higher is the maximum shear stress especially at the lap ends. A 20% increase in the maximum

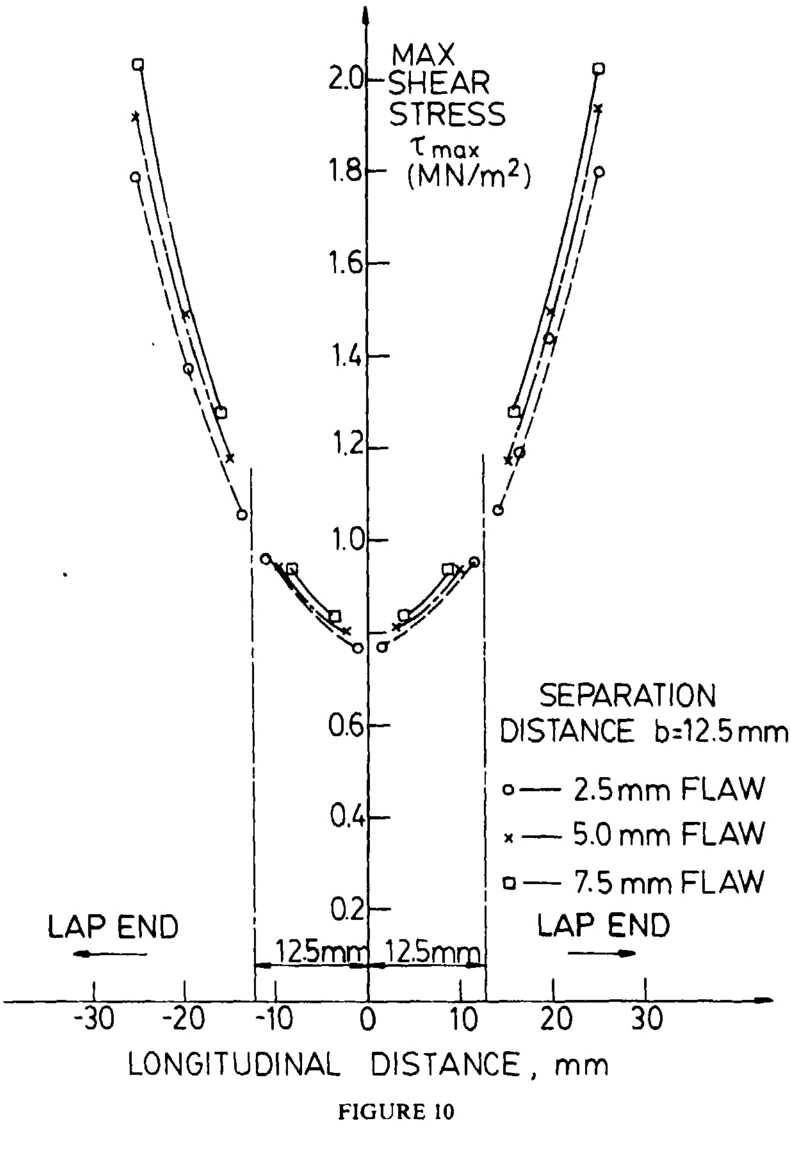

MAX SHEAR STRESS τ_{max} (MN/m^2)
2.0
1.8
1.6
1.4
1.2
1.0
0.6
0.4
0.2
SEPARATION DISTANCE b=12.5 mm
2.5 mm FLAW
5.0 mm FLAW
7.5 mm FLAW
LAP END
LAP END
12.5mm
12.5mm
-30
-20
-10
0
10
20
30
LONGITUDINAL DISTANCE, mm

FIGURE 10

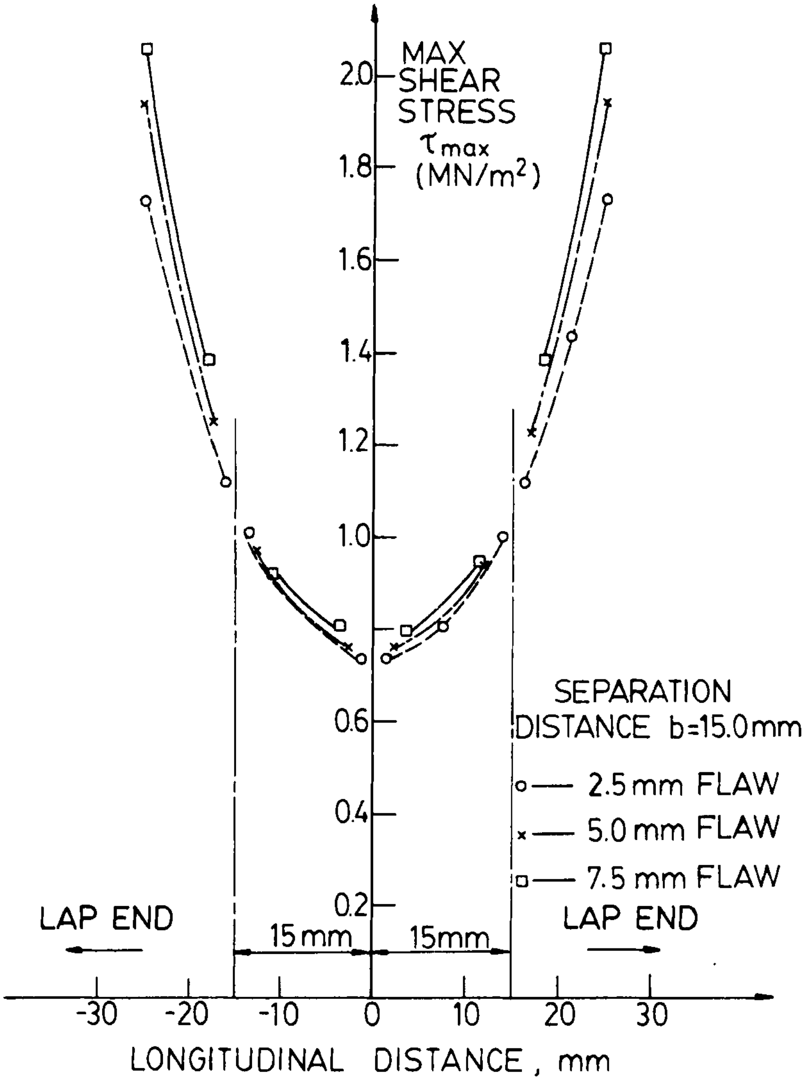

MAX SHEAR STRESS τ_{max} (MN/m²)
2.0
1.8
1.6
1.4
1.2
1.0
0.6
0.4
0.2
SEPARATION DISTANCE b=15.0mm
2.5 mm FLAW
5.0 mm FLAW
7.5 mm FLAW
LAP END
LAP END
15 mm
15mm
-30
-20
-10
0
10
20
30
LONGITUDINAL DISTANCE, mm

FIGURE 11

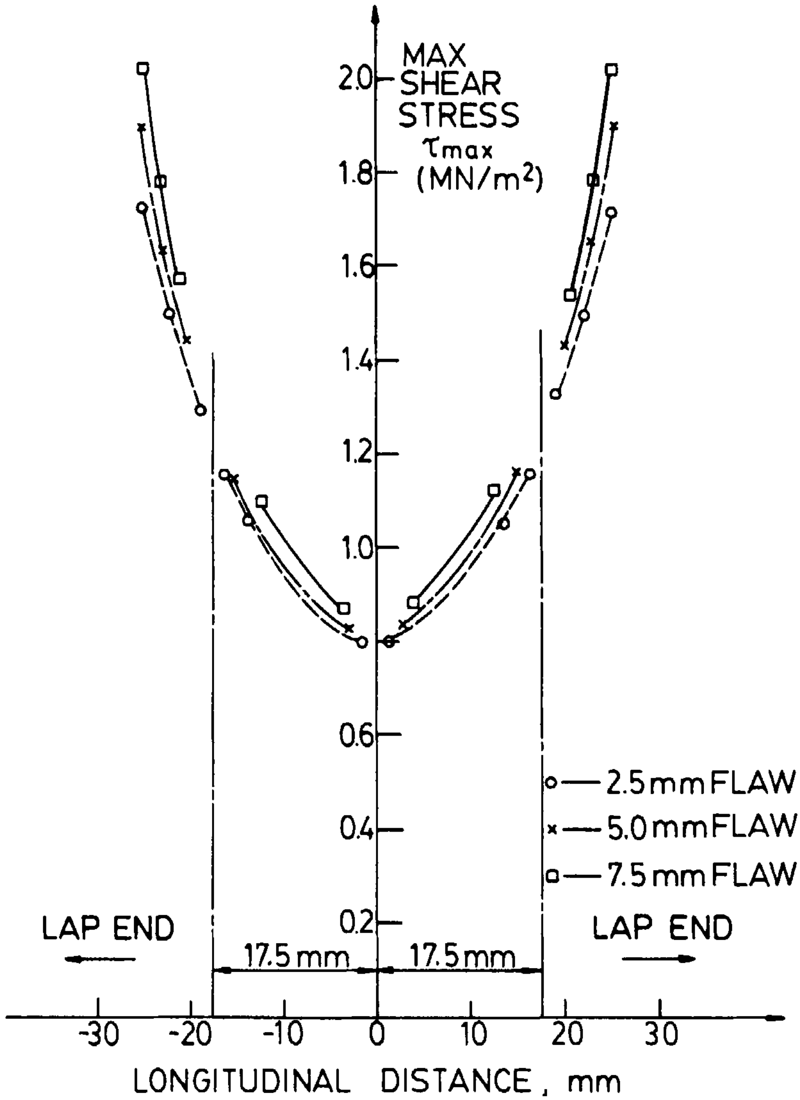
MAX
SHEAR
STRESS
τmax
(MN/m2)
2.0
1.8
1.6
1.4
1.2
1.0
0.6
0.4
0.2
2.5mmFLAW
5.0mmFLAW
7.5mmFLAW
LAP END
LAP END
17.5mm
17.5mm
-30
-20
-10
0
10
20
30
LONGITUDINAL DISTANCE, mm

FIGURE 12

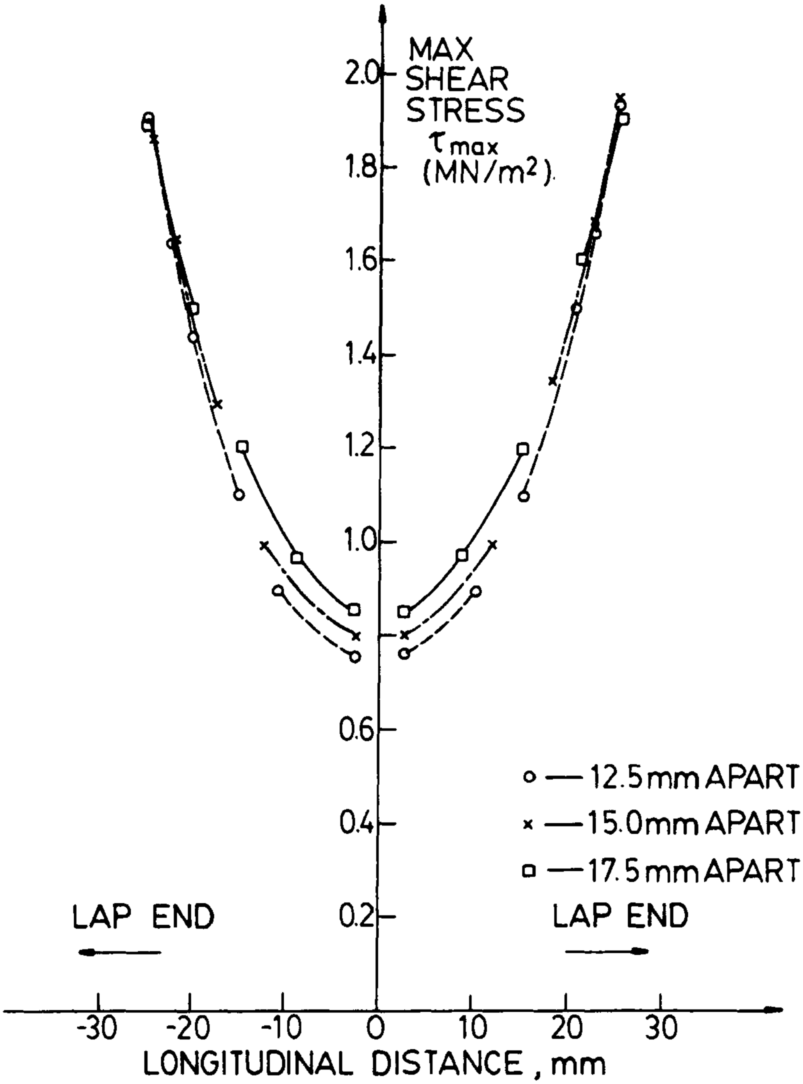
MAX
SHEAR
STRESS
τ max
(MN/m²)
2.0
1.8
1.6
1.4
1.2
1.0
0.6
0.4
0.2
o — 12.5 mm APART
× — 15.0 mm APART
□ — 17.5 mm APART
LAP END
LAP END
-30
-20
-10
0
10
20
30
LONGITUDINAL DISTANCE, mm

FIGURE 13

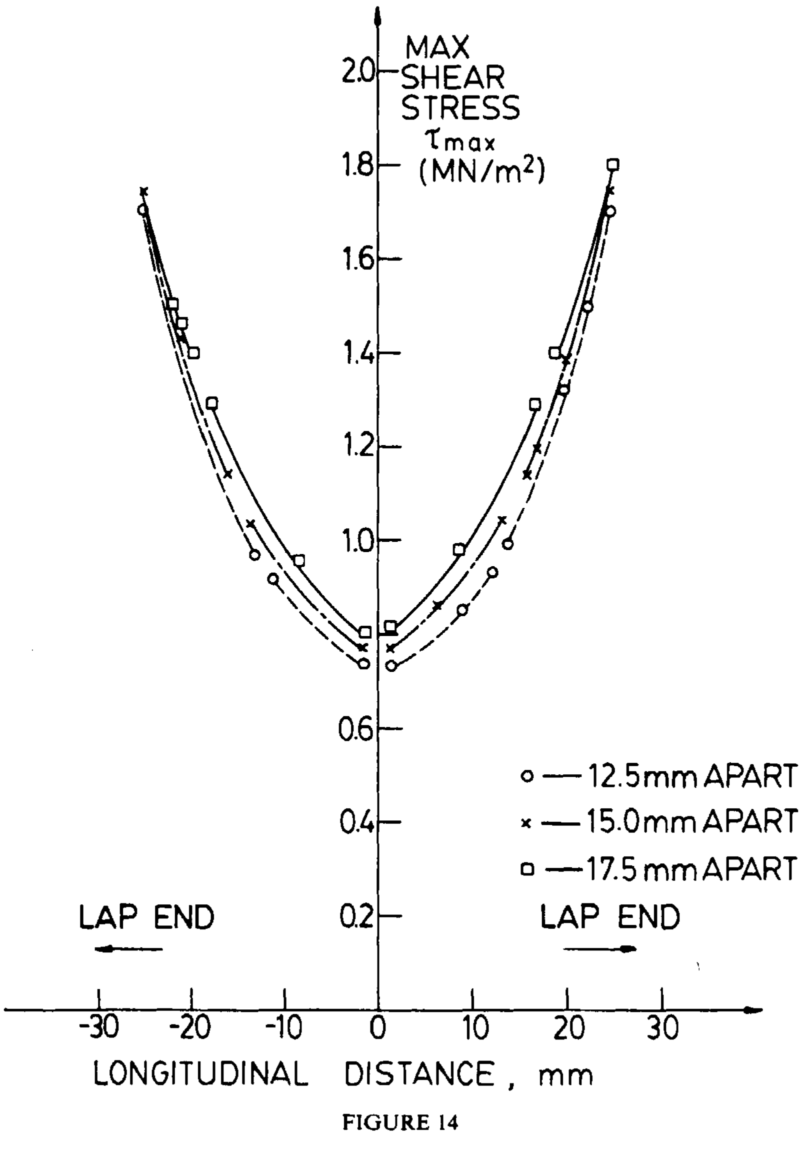
MAX
SHEAR
STRESS
τ_{max}
(MN/m²)
2.0
1.8
1.6
1.4
1.2
1.0
0.6
0.4
0.2
○ — 12.5mm APART
× — 15.0mm APART
□ — 17.5 mm APART
LAP END
LAP END
-30
-20
-10
0
10
20
30
LONGITUDINAL DISTANCE, mm

FIGURE 14

shear stress was observed at the lap end when an isolated central flaw of 5.0 mm was extended to 37.5 mm representing a flaw size of 75% of the lap length.

The shear stress distributions for the lap joint containing three internal flaws were next measured. The shear stress distributions for the lap joint each with a constant flaw separation distance b varying from 12.5 mm, 15 mm and 17.5 mm are shown respectively in Figures 10, 11 and 12. In each figure, the flaw size was varied at 2.5 mm, 5.0 mm and 7.5 mm. It can be observed from the figures that there is negligible effect of flaw separation distance on the maximum shear stress distribution along the adhesive lap joint.

The maximum shear stress distributions for three flaw sizes of 2.5 mm, 5.0 mm and 7.5 mm were next measured and shown respectively in Figures 13, 14 and 15. For each constant flaw size, the flaw separation distance, b, was varied at 12.5 mm, 15 mm and 17.5 mm. It can be observed from the figures that there is no significant effect of flaw separation distance on the maximum shear stresses at the lap ends. There is, however, a significant effect of flaw size on the measured maximum shear stresses. The effect is most pronounced at the lap ends where the maximum shear stress increased up to 45% when the flaw size was lengthened from 2.5 mm to 7.5 mm.

3.2 Adhesively-bonded Aluminium Lap Joints

With the conclusions deduced quantitatively from the photoelastic shear stress measurement, a series of tests were performed to examine the applicability of the photoelastic results on similar lap joints but the adherend was made of aluminium alloy 2024. This material was chosen because of its relevance in aerospace applications. Instead of the shear stress distribution, the fracture strength was measured in order to examine the load-carrying capacity of such lap joints. The fracture strength is defined as the maximum shear load divided by the effective bonded cross-sectional area which is the total bonded area minus the embedded flaws.

Similar investigation into the effect of flaw size variation and its distribution was then undertaken. An initial series of testing consisted of lap specimens with an internal flaw size of 2 mm located at various positions along the lap length. A second series consisted of lap specimens with different flaw sizes located at the centre of the lap. The flaw size to lap length ratio varied from 4% to 50% of the total bonding

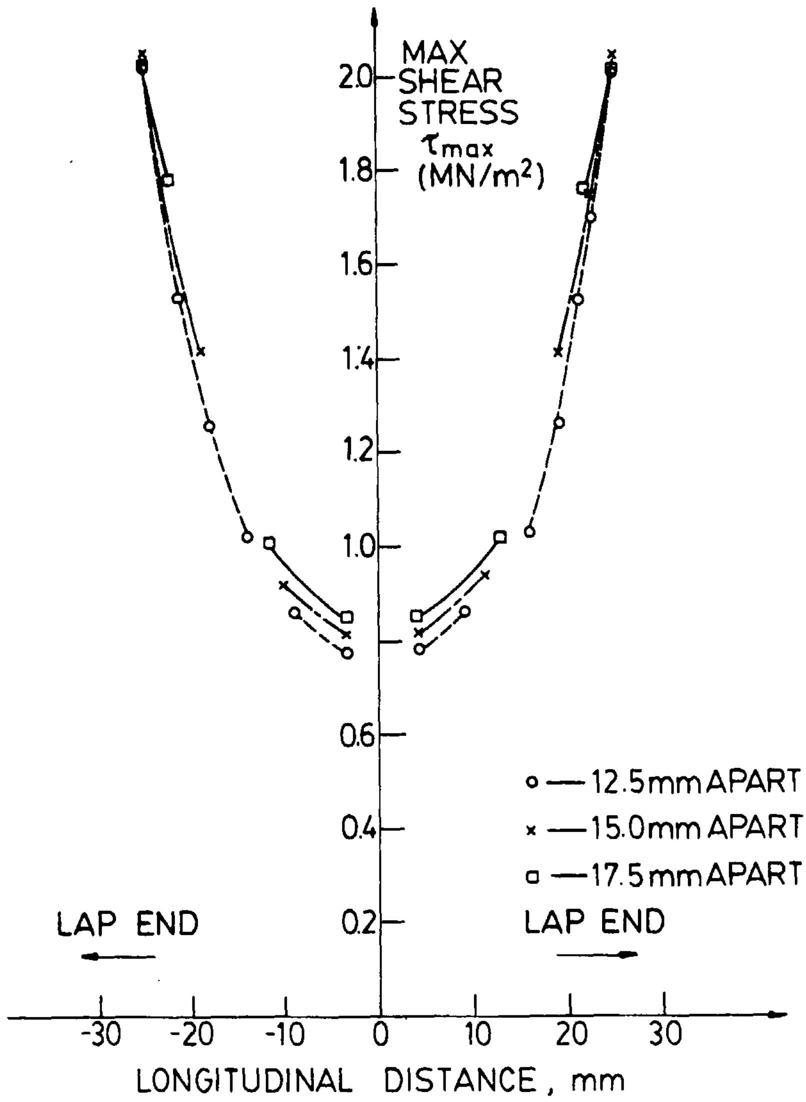
MAX
SHEAR
STRESS
τmax
(MN/m2)
2.0
1.8
1.6
1.4
1.2
1.0
0.6
0.4
0.2
LAP END
LAP END
o —12.5mm APART
× —15.0mm APART
□ —17.5mm APART
-30
-20
-10
0
10
20
30
LONGITUDINAL DISTANCE, mm

FIGURE 15

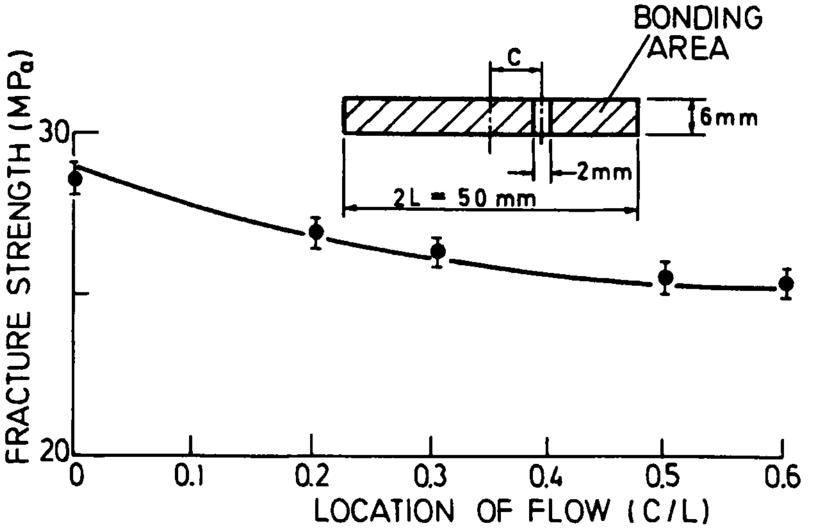

FIGURE 16

lap. The bonded lap length and the adhesive thickness of all the test specimens were kept constant at 50 mm and 0.1 mm respectively. At least three specimens were used in each case in order to ensure repetability of the results.

The aluminium specimens were also prepared with due care. The bonding surfaces were polished with grade 180 emery paper, and then thoroughly degreased and cleaned with acetone before the adhesive was applied. Internal flaws were implanted in the adhesive layer using the same technique as employed in preparing the photoelastic models. The adhesive used for the aluminium bonded joints was CIBA Rapid Araldite as for the photoelastic models. The specimen was then properly cured in an oven for at least 30 minutes at 100°C before being allowed to cool down slowly to room temperature (20°C) at which the testing was carried out. An Instron universal testing machine was used to measure the fracture load at a loading rate of 5 mm/min. The load-displacement record obtained from the autographic recorder was used to calculate the fracture strength.

Figures 16 and 17 summarize the effects of flaw size and its location

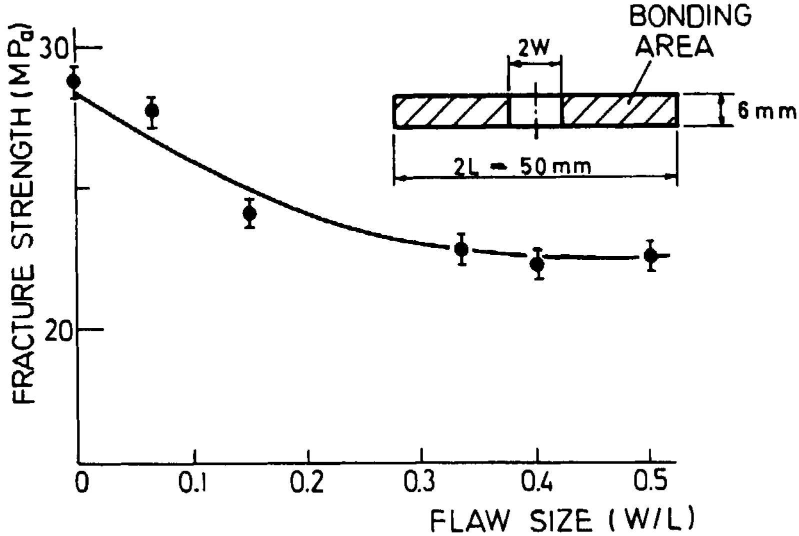

FIGURE 17

on the fracture strength. It can be observed from Figure 16 that the fracture strength is reduced by about 18% when the flaw size is increased to about 50% of the lap length. The flaw distribution is also found to affect the fracture strength as shown in Figure 17. It can be observed from the figure that with a flaw close to the lap end, the fracture strength is reduced by about 12%. The observations from this series of tests indicated that the presence of internal flaw distribution has definite effects on the bonding strength. This conclusion is in qualitative agreement with the photoelastic measurements although the ratio of the Young's modulus of adhesive and adherend is vastly different between the aluminium and photoelastic models.

4. CONCLUSIONS

1. Photoelasticity can be used effectively to quantify the effects of internal flaw distribution on the fracture behaviours of lap joints.
2. Contrary to Renton's conclusion, the lap joint model proposed produced significant normal stresses along the adhesive layer close to the lap ends. This yields difference in the maximum shear stresses

and the transverse shear stresses along the bonding line.

3. There was no significant effect of creep and relaxation of the lap joint on the maximum shear stresses.
4. From all the flaw sizes chosen for the investigation, general profile of maximum shear stress distribution remained similar. However, the larger the flaw size, the higher the maximum shear stresses were observed at the lap free ends.
5. A 20% increase in the maximum shear stress was observed at the lap ends when an isolated central flaw of 5.0 mm was extended to 37.5 mm representing a flaw size 75% of the lap length.
6. For the case of lap joints containing multiple flaws, there is no significant effect of flaw separation distance on the maximum shear stresses along the bonding line.
7. There is a marked increase in the maximum shear stresses up to about 45% at the lap ends when the size of multiple flaws is increased from 2.5 mm to 7.5 mm.

References

1. M. Goland and E. Reissner, *J. Appl. Mechanics, Transactions of ASME* **77**, 17 (1944).
2. K. E. Hahn and D. F. Fouser, *J. Appl. Polym. Sci.* **6**, 145–149 (1962).
3. L. H. Sharpe, "Adhesive Bonding", *Machine Design*, (Sept. 1969), pp. 119–128.
4. F. Erdogan and M. Ratwani, *J. Composite Materials.* **5**, 378–393 (1971).
5. D. J. Chang and R. Muki, *Intern. J. of Solids and Structures* **10**, 503–517 (1974).
6. R. D. Adams and N. A. Peppiatt, *J. of Strain Analysis* **9**(3), 185–196 (1974).
7. S. DasGupta and S. P. Sharma, "Stresses in an Adhesive Lap Joint", ASME publication 75-WA/DE-18, (1975).
8. W. J. Renton, *Experimental Mechanics*, 409–415 (1976).
9. E. Sancaktar and P. D. Lawry *Adhesion*, **11**, 233–241 (1980).
10. U. Youecoglu and D. P. Updike, *J. Engineering Mechanics Division, ASCE*, **EMI**, 55–76 (1981).
11. S. Mostovoy, E. J. Ripling and C. F. Bersch, *J. Adhesion* **3**, 125–144 (1971).
12. E. J. Ripling, S. Mostovoy and H. T. Corten, *ibid.* **3**, 107–123 (1971).
13. S. Mostovoy and E. J. Ripling, *J. App. Polym. Sci.* **15**, 641–659 (1971).
14. G. G. Trantina, *J. Composite Materials* **6**, 192–207 (1972).
15. G. G. Trantina, *Ibid.* **6**, 371–385 (1972).
16. S. S. Wang, J. F. Mandell and F. J. McGarry, *Int. J. Fracture* **14**, 39–58 (1978).
17. C. L. Chow, C. W. Woo and J. L. Sykes, *J. Strain Analysis in Design Engineering* **4**, 37–42 (1979).
18. C. L. Chow and K. M. Ngan, *ibid.* **15**, 97–101 (1980).
19. K. Ikegami and K. Kamiya, *J. Adhesion* **11**, 1–17 (1982).
20. S. Amijma and T. Fujui, in *Fracture Mechanics and Technology* G. C. Sih and C. L. Chow, Eds. 1977), pp. 363–372.
21. A. J. Kinloch, *J. Mat. Sci.* **15**, 2141–2166 (1980).
22. A. J. Kinloch, *ibid.* **17**, 617–651 (1982).
23. J. J. Bikerman, *The Science of Adhesive Joints* (Academic Press, New York, 1961).